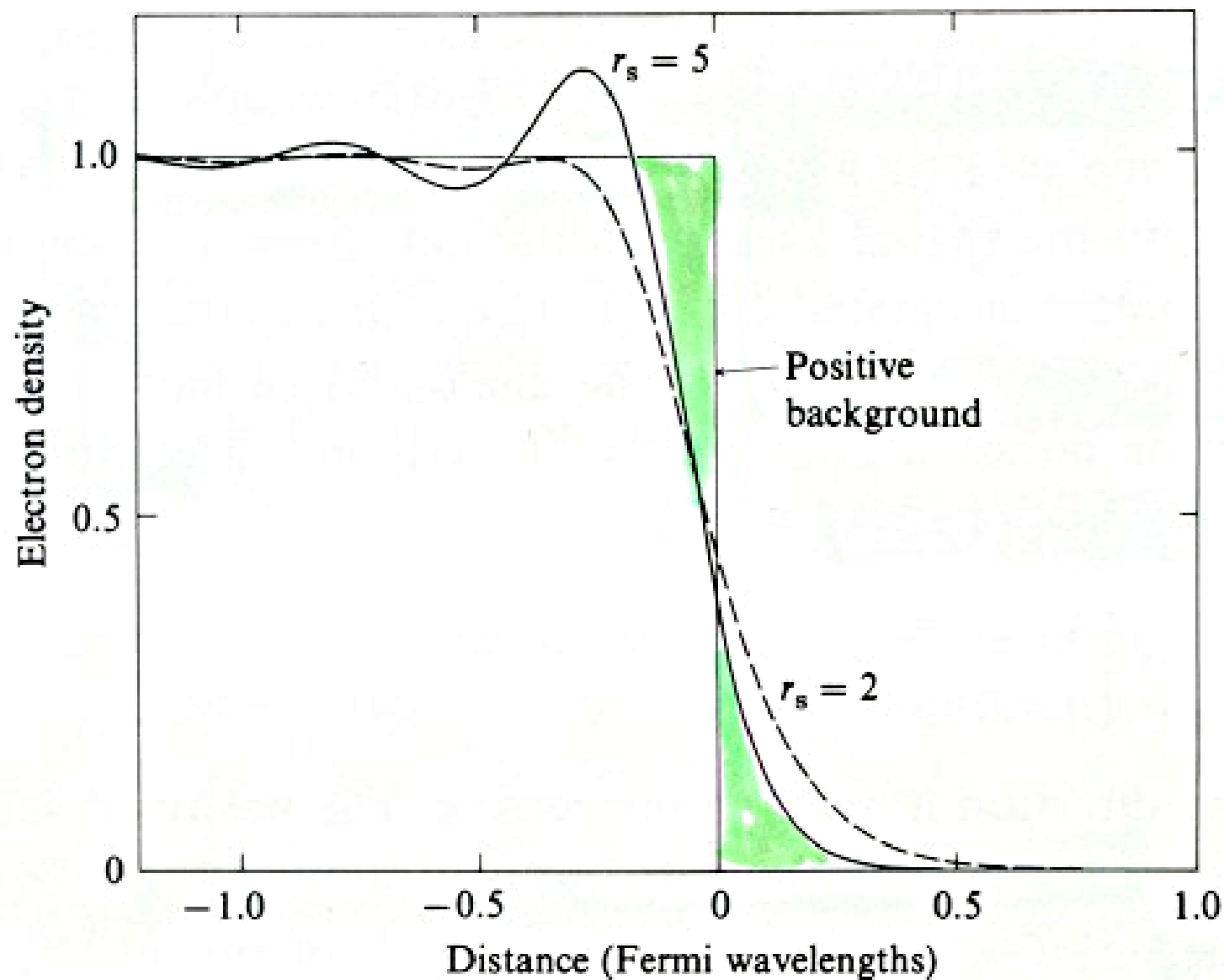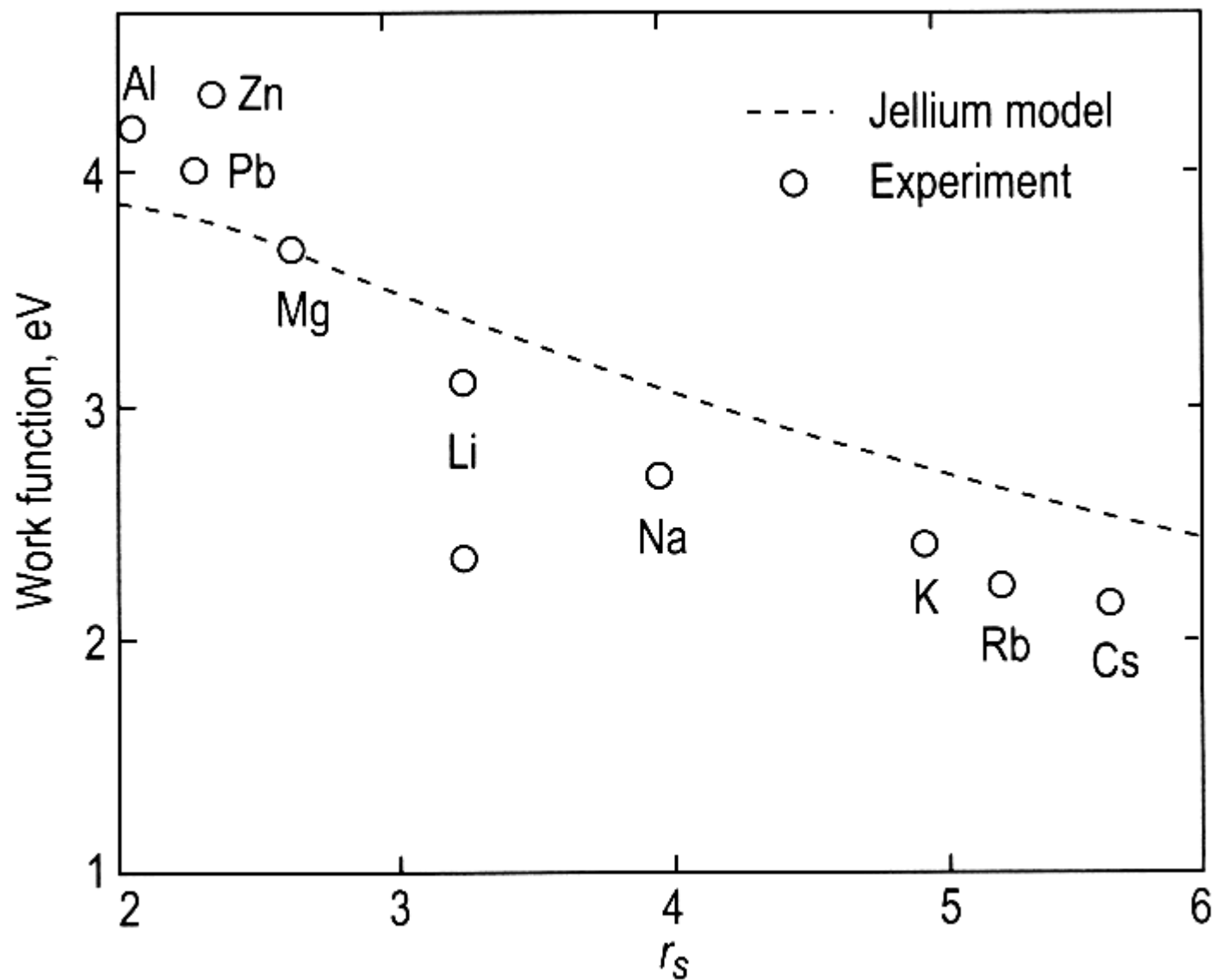Fig. 4.1. Schematic representation of the local density approximation.
$v_{xc}(\mathbf{x}_1) = v_{xc}[n(\mathbf{x}_1)]$ and $v_{xc}(\mathbf{x}_2) = v_{xc}[n(\mathbf{x}_2)]$.

Fig. 4.2. Electron density profile at a jellium surface for two choices of the background density, r_s (Lang & Kohn, 1970).

Fig. 11.4. Experimentally determined work functions (open circles) compared with the results of the Jellium model calculation shown by the dashed line (after Lang and Kohn [11.5])

Fig. 4.3. Electrostatic potential, $v(z)$, and total effective one-electron potential, $v_{\text{eff}}(z)$, near a jellium surface (Lang & Kohn, 1970).
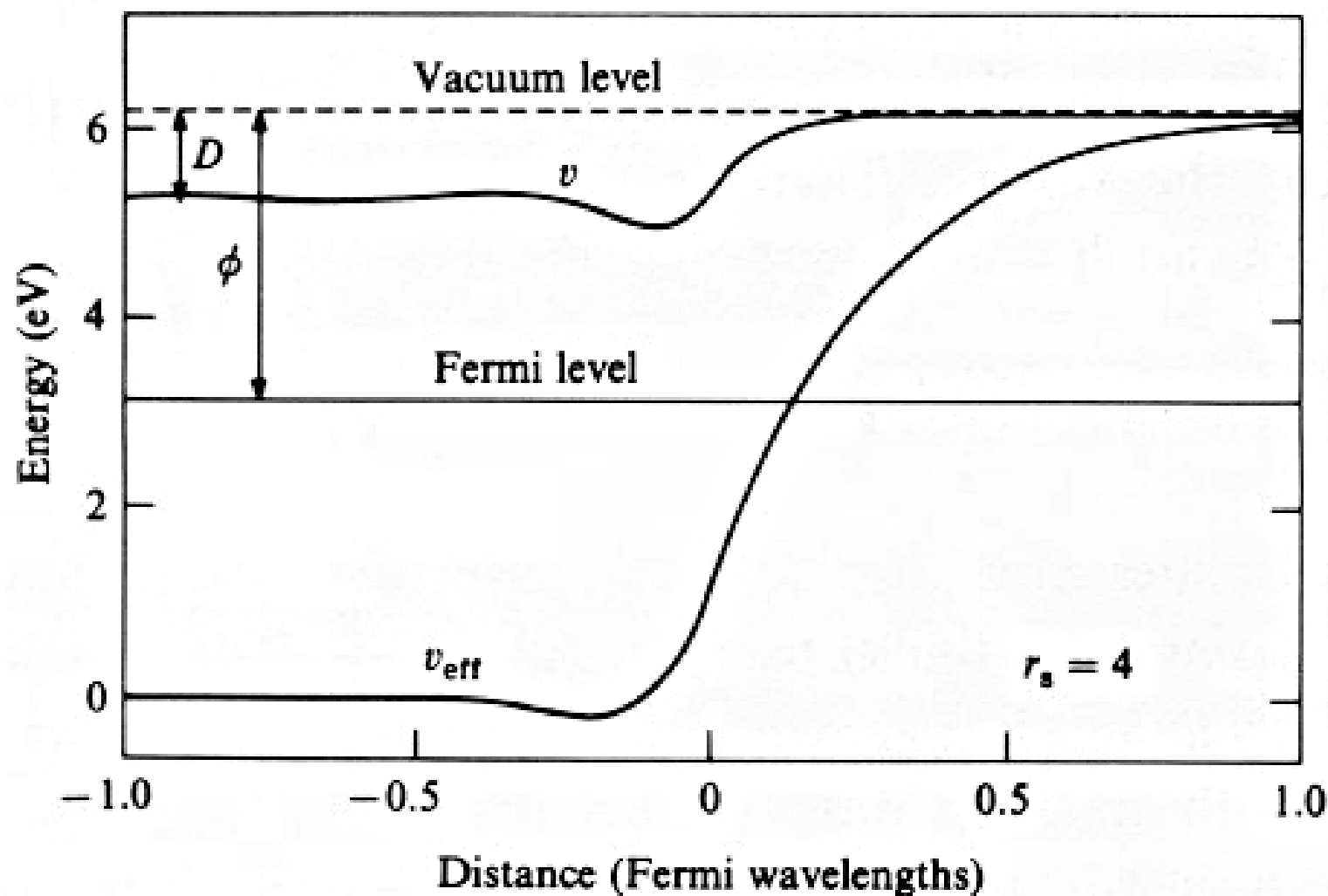
Fig. 4.4. Electrostatic potential near a jellium step. The smoothed electron 'surface', $d_\parallel(x)$, is indicated by the heavy solid curve (Thompson & Huntington, 1982).
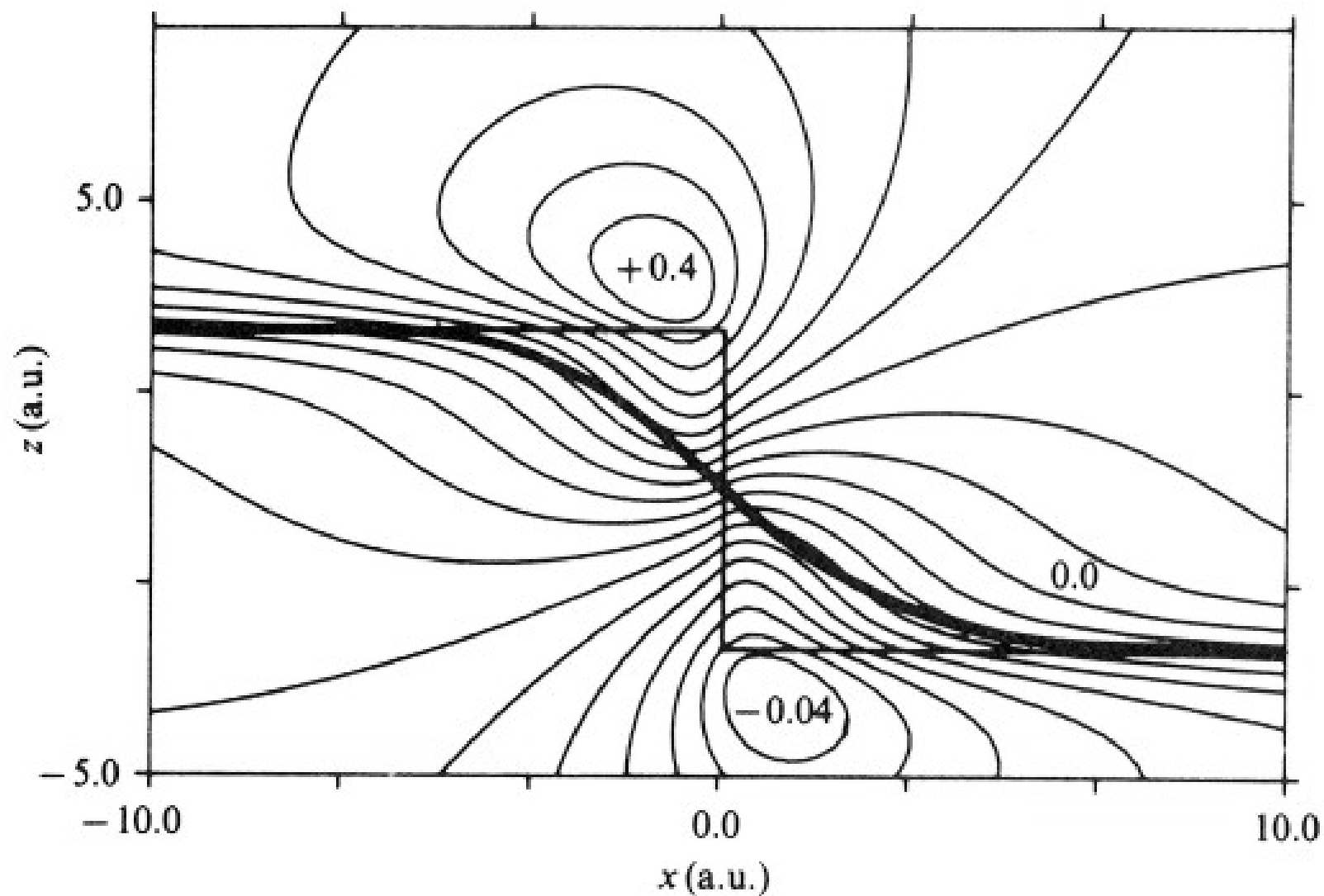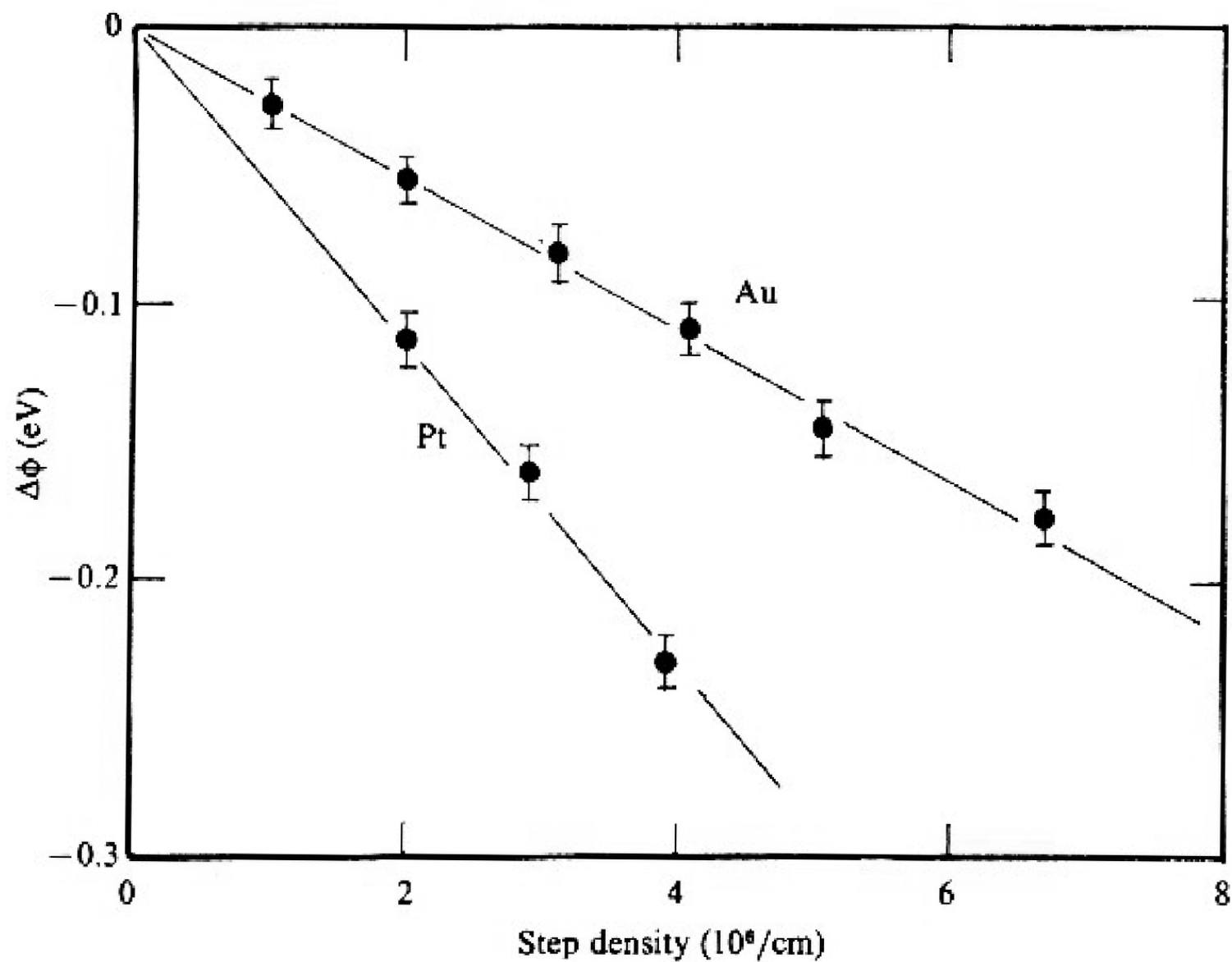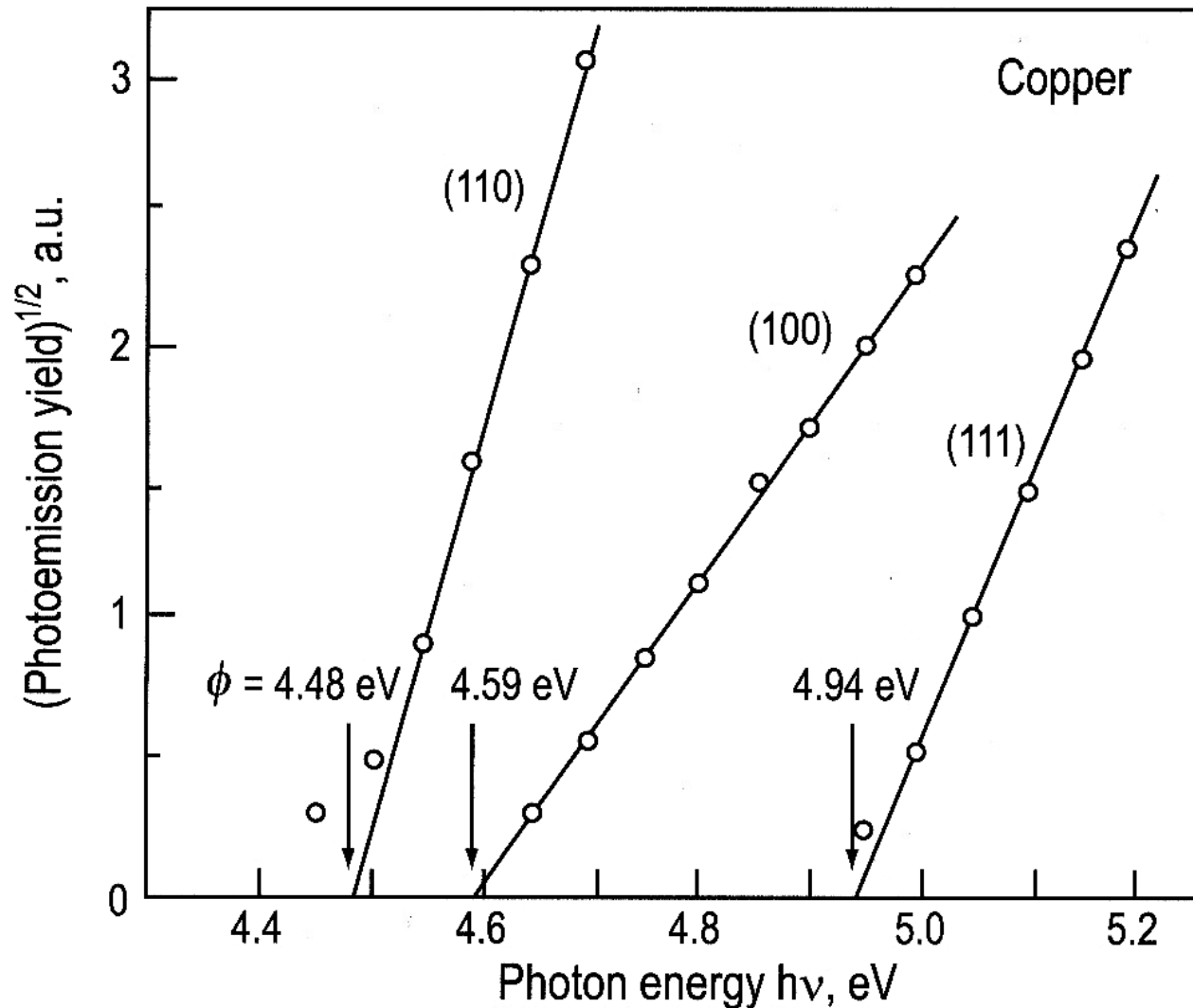
Fig. 4.5. Work function change for stepped metal surfaces (Besocke, Krahl-Urban & Wagner, 1977).
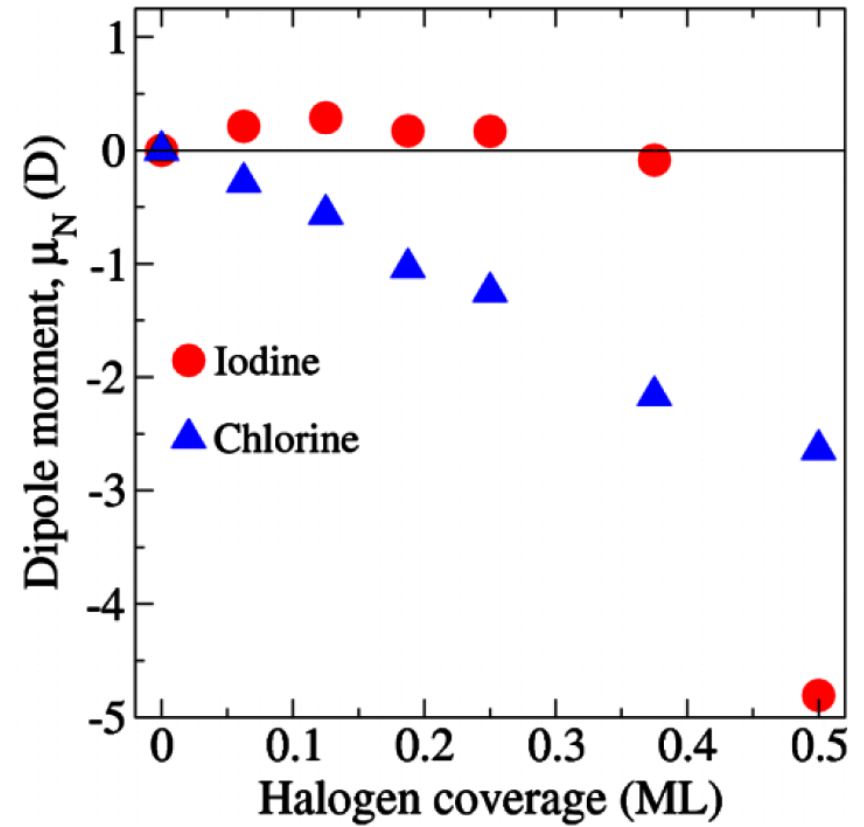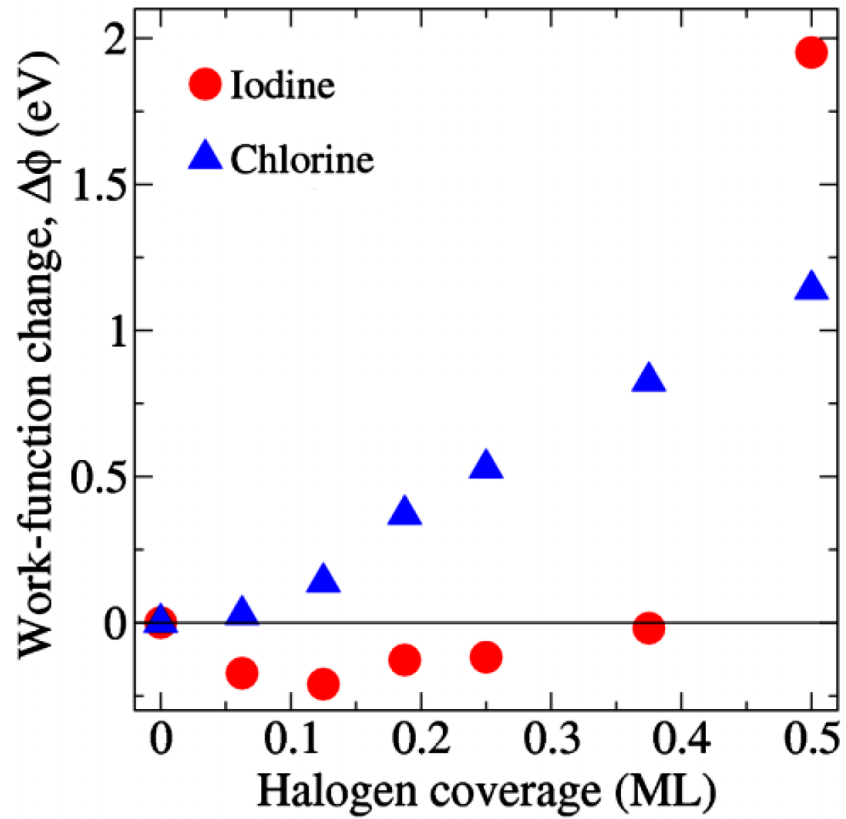
Fig. 11.25. Square root of photoelectric yield as a function of photon energy for selected faces of a Cu crystal. The intercept of the extrapolated dependence with the abscissa yields the value of the work function with an estimated accuracy of ± 0.03 eV (after Gartland et al. [11.35])
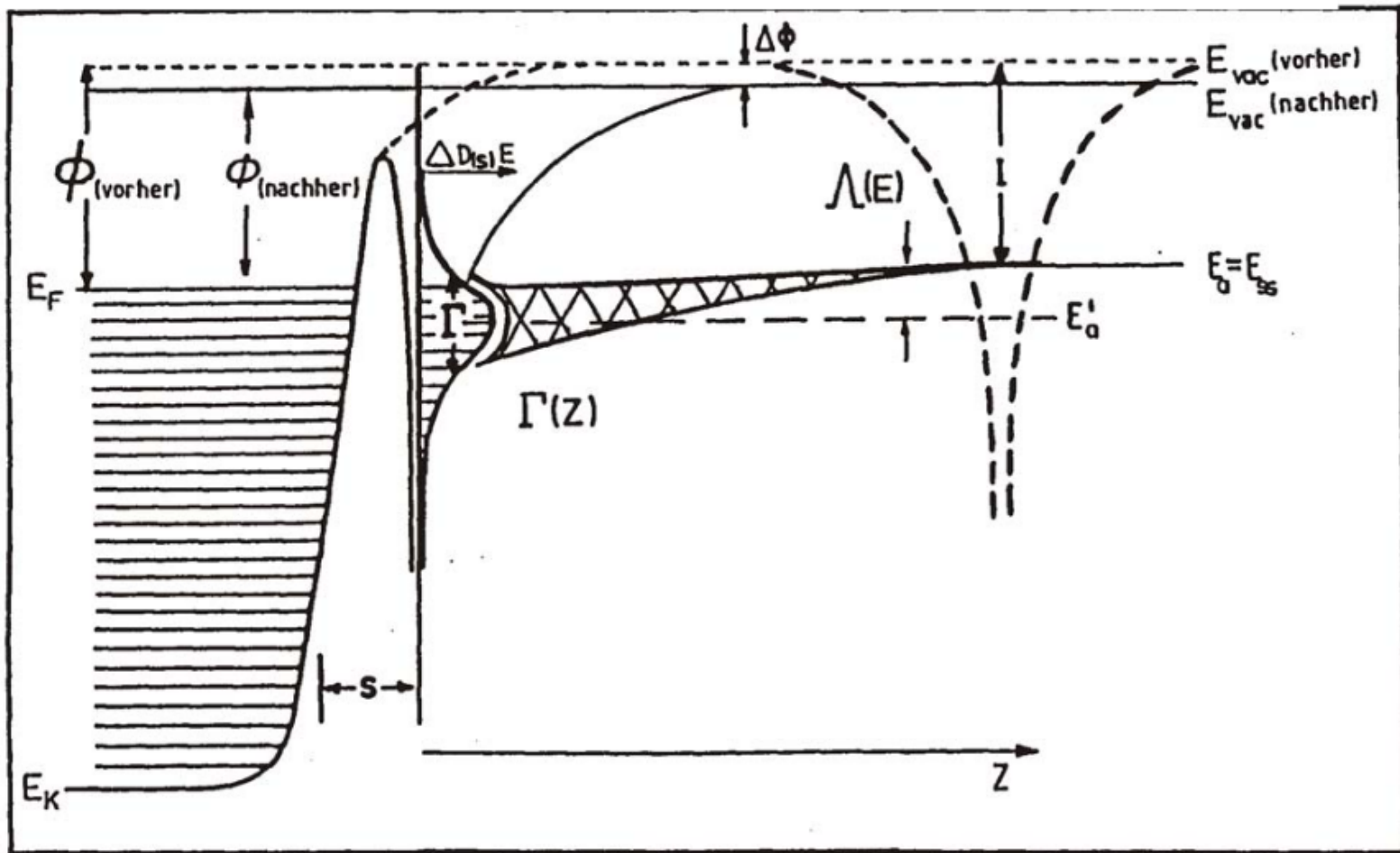
Work-Function Change Induced by Halogens on Cu(111)

Abb. 5.6.13
Schematische Darstellung der Wechselwirkung eines Atoms mit einer Metalloberfläche. Das Atomniveau wird um $\Lambda(E)$ von E_a nach E_a' verschoben und ist im Abstand s um Γ verbreitert. Als Folge der Chemisorption tritt eine Austrittsarbeitsänderung $\Delta\Phi$ auf.

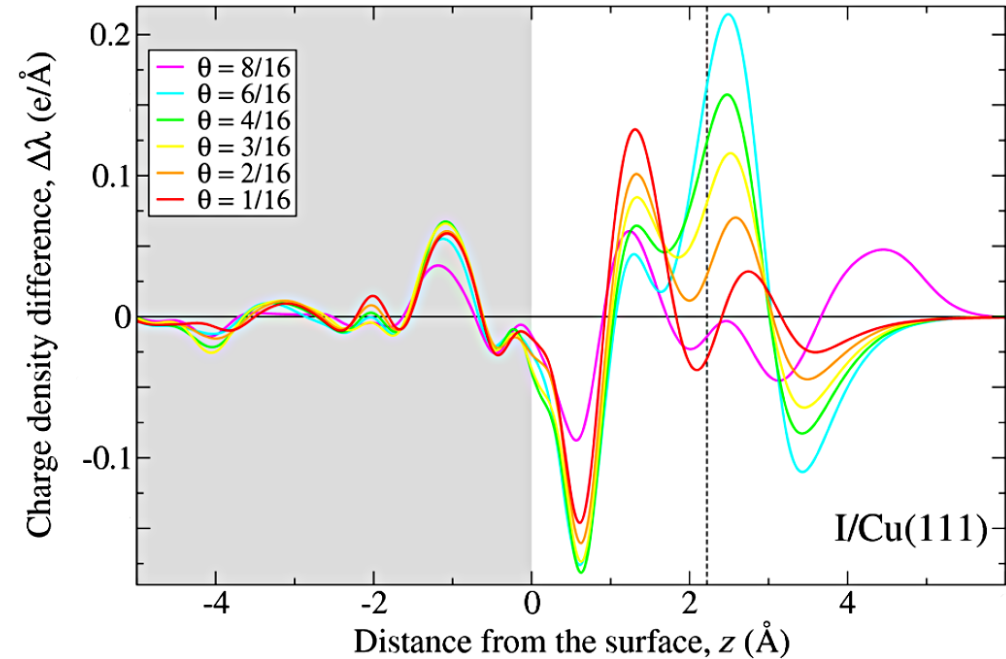# Work-Function Change Induced by Halogens on Cu(111)

Chlor

Jod
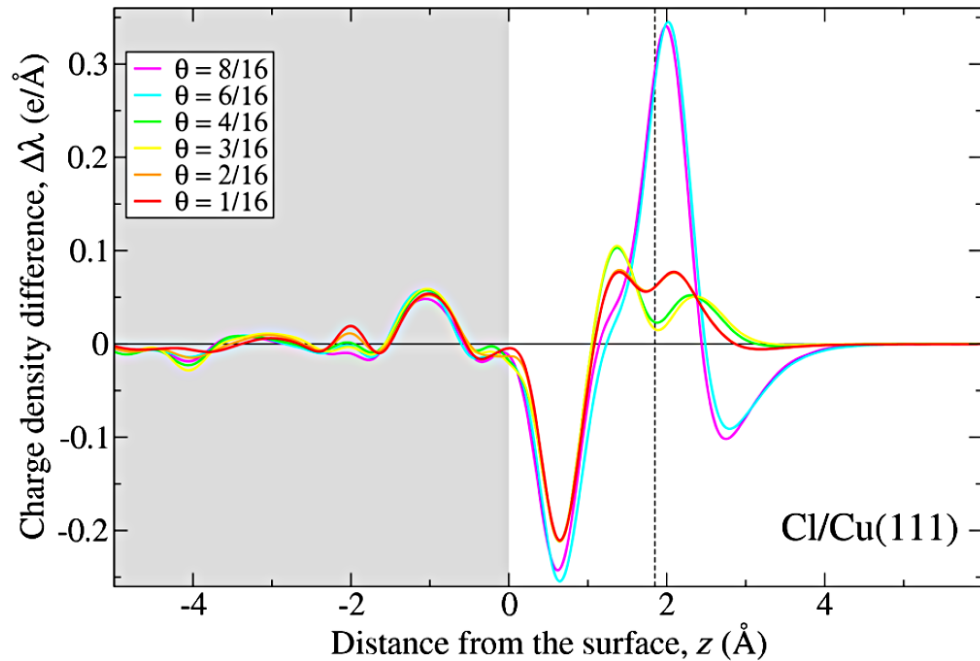
Cl: nahezu perfekte Dipollage

J: groß, polarisierbar

teilkovalente Bindung zu Cu

komplexe Ladungsdichte

Fig. 9.11. Contours of constant charge density for Cl, Si and Li atoms adsorbed on a jellium substrate: (a) total charge; (b) induced charge. Solid (dashed) curves denote a surfeit (depletion) of electrons (Lang & Williams, 1978).

Zangwill, page 217